

Vortex State in $\text{Na}_x\text{CoO}_2 \cdot y\text{H}_2\text{O}$: $p_x \pm ip_y$ -wave versus $d_{x^2-y^2} \pm id_{xy}$ -wave Pairing

Qiang Han^{1,2}, Z. D. Wang^{1,2,*}, Qiang-Hua Wang³, and Tianlong Xia¹

¹*Department of Physics, University of Hong Kong, Pokfulam Road, Hong Kong, China*

²*Department of Material Science and Engineering, University of Science and Technology of China, Hefei Anhui 230026, China and*

³*National Laboratory of Solid State Microstructures, Institute for Solid State Physics, Nanjing University, Nanjing 210093, China*

(Dated: October 5, 2018)

Based on an effective Hamiltonian specified in the triangular lattice with possible $p_x \pm ip_y$ - or $d_{x^2-y^2} \pm id_{xy}$ -wave pairing, which has close relevance to the newly discovered $\text{Na}_{0.35}\text{CoO}_2 \cdot y\text{H}_2\text{O}$, the electronic structure of the vortex state is studied by solving the Bogoliubov-de Gennes equations. It is found that $p_x \pm ip_y$ -wave is favored for the electron doping as the hopping integral $t < 0$. The lowest-lying vortex bound states are found to have respectively zero and positive energies for $p_x \pm ip_y$ - and $d_{x^2-y^2} \pm id_{xy}$ -wave superconductors, whose vortex structures exhibit the intriguing six-fold symmetry. In the presence of strong on-site repulsion, the antiferromagnetic and ferromagnetic orders are induced around the vortex cores for the former and the latter, respectively, both of which cause the splitting of the LDOS peaks due to the lifting of spin degeneracy. The microscopic STM and the spatially resolved NMR measurements are able to probe the new features of vortex states uncovered in this work.

PACS numbers: 74.20.Rp, 74.25.Jb, 74.20.-z

The recent discovery of superconductivity in the Co oxide, $\text{Na}_{0.35}\text{CoO}_2 \cdot y\text{H}_2\text{O}$ [1], has intrigued much interest on its novel properties especially the similarities to and differences from the high- T_c copper oxides. Superconductivity occurs after sodium content is reduced in $\text{Na}_{0.75}\text{CoO}_2$ and the distance between the CoO_2 planes is enlarged by hydration, indicating that the superconductivity is mostly relevant to the two-dimensional CoO_2 layer similar to the role of CuO_2 layers in cuprates. Furthermore, the Co^{4+} atoms in neutral (undoped) CoO_2 plane has spin- $\frac{1}{2}$, resulting in the parent compound a spin- $\frac{1}{2}$ antiferromagnet. On the other hand, because the spins form a triangular lattice, the antiferromagnetism is frustrated and the resonating-valence-bond (RVB) state [2] might give rise to superconductivity under proper doping. At present, the mechanism of the superconductivity in this material is hotly debated and accordingly the pairing symmetry of the superconducting order parameter (OP) has been paid significant attention although still controversial. Theories [3, 4, 5] based on the RVB theory support the view that the superconducting OP has the spin-singlet broken-time-reversal-symmetry (BTRS) chiral $d_{x^2-y^2} \pm id_{xy}$ symmetry, while theories based on a combined symmetry analysis with fermiology [6] and numerical calculations [7, 8] of normal state electronic structure speculate that the OP is spin-triplet BTRS chiral $p_x \pm ip_y$ -wave symmetry. The experimental results reported by different groups using the same nuclear-magnetic-resonance(NMR) technique are also confusing: one group [9] supports the spin-triplet $p_x + ip_y$ -wave symmetry while another group [10] claimed to support the spin-singlet s -wave symmetry.

In this Letter, to have valuable clues for experimental clarification, we elucidate and compare the effects of the

two most possible pairing symmetries, $p_x + ip_y$ [6, 7, 8] and $d_{x^2-y^2} + id_{xy}$ [3, 4, 5] waves, on the electronic structure of the vortex state. In particular, we shall answer two crucial questions clearly: (i) what are the new features of the vortex state in this kind of triangular system? (ii) what are the experimentally observable signatures showing the differences between the mentioned two pairing symmetries? Because the mechanism of the superconductivity in $\text{Na}_{0.35}\text{CoO}_2 \cdot y\text{H}_2\text{O}$ is still unclear at present, we will not adopt the well-known t - J model as in Refs. [4, 5] as it only gives rise to the spin-singlet pairing. Here the well-established t - U - V Hubbard model [11] is employed with competing magnetic (U) and superconducting (V) interactions. Although phenomenological, this model captures the rich physics of system with competing orders and has been applied to study the field-induced antiferromagnetic and charge-density-wave (CDW) orderings around the vortex core of high- T_c d -wave cuprates[12], having accounted for several important experimental observations. Considering similarities of this new superconductor to the cuprates as well as possibilities of both spin singlet and triplet pairings, we extend this model to study the superconducting cobalt oxide with either spin singlet or triplet pairing channel in the triangular lattice and examine the novel properties in the vortex state. The effective model Hamiltonian is expressed as

$$H_{\text{eff}} = - \sum_{\langle i,j \rangle \sigma} (t_{ij} c_{i\sigma}^\dagger c_{j\sigma} + \text{h.c.}) + \sum_{i,\sigma} (U n_{i\sigma} - \mu) c_{i\sigma}^\dagger c_{i\sigma} + \sum_{\langle i,j \rangle} \left[\Delta_{ij}^\pm (c_{i\uparrow}^\dagger c_{j\downarrow}^\dagger \pm c_{i\downarrow}^\dagger c_{j\uparrow}^\dagger) + \text{h.c.} \right], \quad (1)$$

where $n_{i\sigma} = \langle c_{i\sigma}^\dagger c_{i\sigma} \rangle$ is the electron density with spin σ . μ is the chemical potential. \pm is for spin triplet

and singlet pairings, respectively and the pairing potential Δ_{ij}^{\pm} is defined as $\Delta_{ij}^{\pm} = \frac{V}{2}(\langle c_{i\uparrow}c_{j\downarrow} \rangle \pm \langle c_{i\downarrow}c_{j\uparrow} \rangle)$, which comes from a mean field treatment of the pairing interaction $V \sum_{\langle i,j \rangle} (c_{i\uparrow}^{\dagger}c_{j\downarrow}^{\dagger}c_{i\uparrow}c_{j\downarrow} + c_{i\downarrow}^{\dagger}c_{j\uparrow}^{\dagger}c_{i\downarrow}c_{j\uparrow})$. In an external magnetic field, the hopping integral t_{ij} can be written as $t_{ij} = t \exp(i\varphi_{i,j})$ for the nearest-neighbor (NN) sites $\langle i,j \rangle$, where $\varphi_{i,j} = -\frac{\pi}{\Phi_0} \int_{\mathbf{r}_i}^{\mathbf{r}_j} \mathbf{A}(\mathbf{r}) \cdot d\mathbf{r}$ with $\mathbf{A}(\mathbf{r})$ the vector potential and $\Phi_0 = hc/2e$ the superconducting flux quantum. The internal field induced by supercurrents around the vortex core is neglected since $\text{Na}_{0.35}\text{CoO}_2 \cdot y\text{H}_2\text{O}$ can be treated as extreme type-II superconductors according to experiment [13] estimation. Therefore, $\mathbf{A}(\mathbf{r})$ is approximated as $(0, Bx, 0)$ in a Landau gauge where B is the external magnetic field. By applying the self-consistent mean-field approximation and performing the Bogoliubov transformation, diagonalization of the Hamiltonian H_{eff} can be achieved by solving the following Bogoliubov-de Gennes (BdG) equations:

$$\sum_j \begin{pmatrix} H_{ij,\sigma} & \Delta_{ij}^{\pm} \\ \mp \Delta_{ij}^{\pm*} & -H_{ij,\bar{\sigma}}^* \end{pmatrix} \begin{pmatrix} u_{j,\sigma}^n \\ v_{j,\bar{\sigma}}^n \end{pmatrix} = E_n \begin{pmatrix} u_{j,\sigma}^n \\ v_{j,\bar{\sigma}}^n \end{pmatrix} \quad (2)$$

where u^n, v^n are the Bogoliubov quasiparticle amplitudes with corresponding eigenvalue E_n . $H_{ij,\sigma} = -t_{ij} + \delta_{i,j}(Un_{i\bar{\sigma}} - \mu)$ with $n_{i\sigma}$ subject to the self-consistent conditions: $n_{i\uparrow} = \sum_n \{|u_{i,\uparrow}^n|^2 f(E_n)\}$ and $n_{i\downarrow} = \sum_n \{|v_{i,\downarrow}^n|^2 [1 - f(E_n)]\}$ with $f(E)$ the Fermi distribution function. $\Delta_{i,j}$ is calculated according to: $\Delta_{i,j}^{\pm} = \frac{V}{4} \sum_n (u_{i\uparrow}^n v_{j\downarrow}^{n*} \mp u_{j\uparrow}^n v_{i\downarrow}^{n*}) \tanh(\frac{E_n}{2k_B T})$.

In this work, we choose such a magnetic unit cell (MUC), which accommodates two superconducting flux quanta $2\Phi_0$ [14] and is characterized by $\mathbf{R}_1 = N\mathbf{a}_1$ and $\mathbf{R}_2 = 2N\mathbf{a}_2$ with N an integer. $\mathbf{a}_1 = a(\sqrt{3}/2, 1/2)$ and $\mathbf{a}_2 = a(0, 1)$ are the prime translation vectors of the CoO_2 triangular lattice. By introducing the magnetic Bloch states labelled by the quasimomentum, we can handle an array of MUC's under the modified periodic boundary condition related to the phase factor by magnetic translations $\chi(\mathbf{r}, \mathbf{R}) = -2\pi m y - \pi(m - 2n + m^2/2)$ with $\mathbf{R} = m\mathbf{R}_1 + n\mathbf{R}_2$. In addition, we set $t < 0$ [15] according to the analysis on the band calculation [3, 5, 7]. The energy and length will be measured in units of $|t|$ and the lattice constant a .

It is noteworthy that the coexistence of and competition between superconductivity and ferromagnetism(FM)/antiferromagnetism(AFM) in this novel material is very interesting and important, but quite complicated even in the homogenous case. We leave it for future careful investigation. In the present work, we focus only on the vortex state, bearing in mind that magnetic orders may be induced in the vortex cores where superconductivity is significantly suppressed. In the homogenous superconducting state, we find that the $p_x \pm ip_y$ -wave pairing state is always favored for $\bar{n} > 1$ while the $d_{x^2-y^2} \pm id_{xy}$ -wave case is stabilized for $0.5 < \bar{n} < 1$ [15] with \bar{n} the average electron number per site.

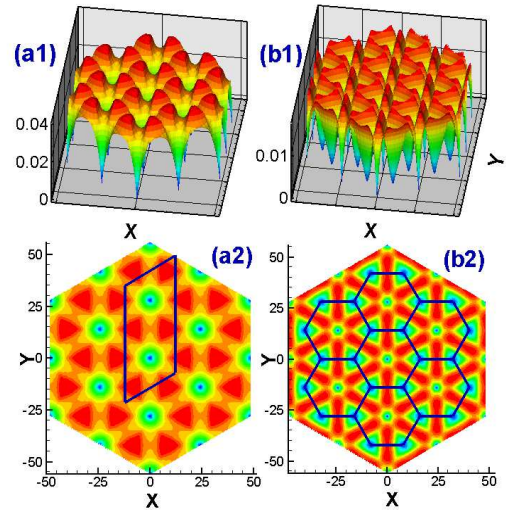


FIG. 1: 3D and contour plots of the spatial distribution of the dominant $|\Delta^{p_x + ip_y}|$ (a) and the induced subdominant $|\Delta^{p_x - ip_y}|$ (b). The blue parallelogram in (a2) denotes the 28×56 MUC in our study. See text for detail.

Now we address the vortex lattice structure of the gauge-invariant $\Delta^{p_x \pm ip_y}$ and $\Delta^{d_{x^2-y^2} \pm id_{xy}}$ according to $\Delta^{p_x \pm ip_y}(\mathbf{r}_i) = \sum_{\delta} \Delta_{i,i+\delta}^{\pm} e^{\mp i\theta(\delta)} e^{i\varphi_{i,i+\delta}}/6$ and $\Delta^{d_{x^2-y^2} \pm id_{xy}}(\mathbf{r}_i) = \sum_{\delta} \Delta_{i,i+\delta}^{\mp} e^{\mp 2i\theta(\delta)} e^{i\varphi_{i,i+\delta}}/6$, where $i+\delta$ denotes the six NN sites of the site i . The energy degeneracy of $\Delta^{p_x \pm ip_y}$ is lifted in the presence of magnetic field and the $\Delta^{p_x + ip_y}$ is energetically favored when the field is applied along \hat{z} , resulting in $\Delta^{p_x + ip_y}(\mathbf{r}) = |\Delta(r)|e^{-i\phi}$ (winding number -1). Combining with our further identification of such behavior in the $d_{x^2-y^2} \pm id_{xy}$ -wave case where $d_{x^2-y^2} + id_{xy}$ is favored, it indicates that the internal phase winding of the Cooper pairs will try to counteract the phase winding of the vortex to save the energy cost of supercurrents. To study the vortex lattice structure of $\Delta^{p_x + ip_y}$, we select a favorable electron occupancy $\bar{n} = 1.2$ and $V = 1.6$, giving rise to the bulk value of $\Delta^{p_x + ip_y} = 0.043$. Such a small OP value results in a gap opened at $\Delta_{\text{Gap}} = 0.14$ with a large core size according to the estimation $k_F \xi \sim 2E_F/\pi\Delta_{\text{Gap}} \simeq 27$. Figure 1 shows the spatial distribution of the dominant $\Delta^{p_x + ip_y}(\mathbf{r})$ together with the induced subdominant $\Delta^{p_x - ip_y}$ component, both with obvious six-fold symmetry. Because the magnitude of $\Delta^{p_x \pm ip_y}$ is small, it is sensitive to the magnetic field, resulting in a large modulation of the magnitude of OP. The induced subdominant $\Delta^{p_x - ip_y}$ is about one third of $\Delta^{p_x + ip_y}$. The spatial structure of the subdominant $\Delta^{p_x - ip_y}$ has some peculiar properties as displayed in Figs. 1(b1) and (b2) which has not been shown before to our knowledge. We find that in addition to the original vortices (OV) [small green disks in Fig. 1(b2), with winding number +1], inter-vortex vortices (IVV) [green triangles in Fig. 1(b2), with winding number -1] are generated within every three OV. Therefore, each OV

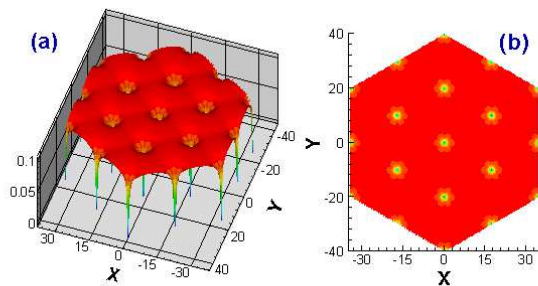


FIG. 2: 3D (a) and contour plots (b) of the spatial distribution of $|\Delta^{d_{x^2-y^2}+id_{xy}}|$. The MUC here is 20×40 .

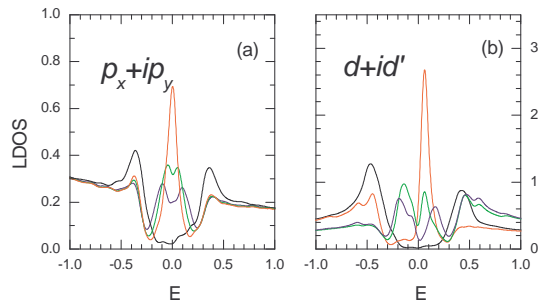


FIG. 3: The LDOS of $p_x + ip_y$ - (a), $d_{x^2-y^2} + id_{xy}$ -wave (b) vortex lattice without ferromagnetic order ($U=0$) at the vortex center (red lines), NN site of vortex center (green lines), next NN site of vortex center (blue lines) and midway of two nearest vortices (black lines). $V = 2$, $\bar{n} = 1.2$ for (a); and $V = 1.3$, $\bar{n} = 0.67$ for (b). The thermal broadening temperature is 0.02.

is surrounded by six IVV and each IVV by three OV and three IVV. The IVV forms honeycomb vortex lattice with length of the side $\frac{1}{\sqrt{3}}$ of that of the OV lattice. A similar behavior has also been found for the $d_{x^2-y^2} \pm id_{xy}$ -wave case. For larger gap values, we study the vortex lattice structure of $\Delta^{d_{x^2-y^2} \pm id_{xy}}$. We choose the electron occupancy $\bar{n} = 0.67$ and $V = 1.3$, which leads to the bulk value of $\Delta^{d_{x^2-y^2}+id_{xy}} = 0.10$ ($\Delta_{\text{Gap}} = 0.4$). The spatial pattern of $|\Delta^{d_{x^2-y^2}+id_{xy}}(\mathbf{r})|$ is shown in Fig. 2. The subdominant $\Delta^{d-id'}$ (not shown here) has a similar structure to $\Delta^{p_x-ip_y}$ [Fig. 1(b)] and the IVV also forms honeycomb vortex lattice structures.

The local density of states (LDOS) as a function of energy of the two pairing states are displayed in Fig. 3 with definition $\rho(\mathbf{r}_i, E) = -\sum_n [|u_{i,\uparrow}^n|^2 f'(E_n - E) + |v_{i,\downarrow}^n|^2 f'(E_n + E)]$, which is proportional to the differential tunnelling conductance observed in scanning tunnelling microscopy (STM) experiments. For clarity, we set $V = 2.0$ with $\bar{n} = 1.2$ to enlarge the $p_x + ip_y$ -wave OP ($\Delta^{p_x+ip_y} = 0.09$) and $V = 1.3$ with $\bar{n} = 0.67$ for the $d_{x^2-y^2} + id_{xy}$ pairing state so that the gaps opened by them are comparable. Note that the LDOS of the $p_x + ip_y$ -wave pairing state is much lower than that of the $d_{x^2-y^2} + id_{xy}$ -wave case because the chemical potential

is sitting on the electronic spectrum position where the density of states of the normal state is low. In the midway between two NN vortices, the LDOS resembles that in bulk: both the chiral $p_x + ip_y$ -wave and $d_{x^2-y^2} + id_{xy}$ -wave pairing states open full gaps. Consequently, the low-lying quasiparticle bound states emerge within the gap as expected, similar to the conventional s -wave vortex core states[16]. However, the energies of the lowest core states in the vortex center of both the $p_x + ip_y$ and $d_{x^2-y^2} + id_{xy}$ -wave pairing states deviate the approximate relation $E_1 = -\Delta_0^2/E_F$ (Note that $t < 0$) for conventional s -wave superconductors. E_1 of $p_x + ip_y$ vortex is zero (pinned on the Fermi level) while that of $d_{x^2-y^2} + id_{xy}$ -wave vortex is positive (above the Fermi level). The difference of the bound state energy between $p_x + ip_y$ - and $d_{x^2-y^2} + id_{xy}$ -wave vortex states is non-trivial and is intrinsic to the internal angular momentum l_z of the Cooper pairs. For the $p_x + ip_y$ -wave state, the quasiparticle wave functions u and v have 0 angular momentum reflecting the total effect of the phase winding -1 of vortex and $l_z = 1$ of Cooper pairs, which accordingly gives rise to a bound state with *strictly zero energy* [17]. Similarly, for the Cooper pair ($l_z = 2$) with $d_{x^2-y^2} + id_{xy}$ -wave pairing symmetry[18], u has 0 and v -1 angular momentum thus with a positive bound energy[17]. This novel difference of vortex core bound states between the two gapped chiral $p_x + ip_y$ and $d_{x^2-y^2} + id_{xy}$ -wave pairing state can be observed by STM experiments with high energy resolution and might help to identify the pairing symmetry in this material.

We then study the induced magnetic moment around the vortex core by examining the magnetization defined as $M_s(\mathbf{r}_i) = n_{i\uparrow} - n_{i\downarrow}$ and its dependence on U and \bar{n} . For the electron-doped case, we find that in the presence of on-site repulsion the frustrated AFM moment might be nucleated near the core for small doping as analogy to the case of cuprates. The magnetic moment at the $p_x + ip_y$ -wave vortex core, M_s^{core} , as a function of U with $\bar{n} = 1.2$ and $\bar{n} = 1.3$ is shown in Fig. 4(a1) with fixed $V = 2.0$. The critical value U_{cr} increases while M_s^{core} decreases with \bar{n} and we find no magnetic moment for large doping with $\bar{n} = 1.4$ up to $U = 5$. And larger V also results in larger U_{cr} because superconductivity competes with magnetism. For the hole-doped region with $\bar{n} < 0.8$, a localized FM (instead of AFM) moment is induced around the $d_{x^2-y^2} + id_{xy}$ -wave vortices, completely different from the picture of field-induced AFM order in high- T_c d -wave superconductors. Fig. 4(b1) displays the U dependence of M_s^{core} for $\bar{n} = 0.6$ and $\bar{n} = 0.7$. Contrary to the electron doped case, larger doping gives rise to weaker U_{cr} and stronger magnetic moment. We find that these seemingly surprising results have little relevance to the pairing symmetry, but are intrinsic to the competition between the AFM and FM orders in our model. The AFM state dominates the region near the half filling, while the FM or paramagnetic metallic states dominates the region near

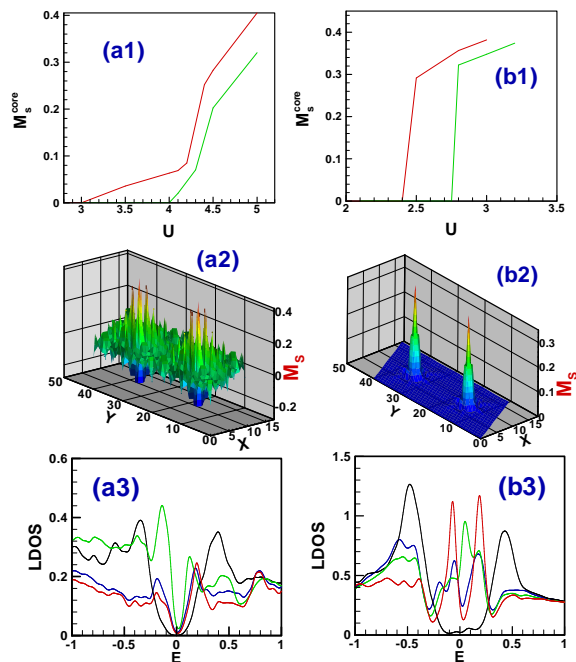


FIG. 4: (a1): The induced AFM moment at the $p_x + ip_y$ -wave vortex core M_s^{core} as a function of U for $\bar{n} = 1.2$ (red) and $\bar{n} = 1.3$ (green). (a2): The spatial structure of M_s with $\bar{n} = 1.2$ and $U = 5$. (b1): The induced FM moment at the $d_{x^2-y^2} + id_{xy}$ -wave vortex core M_s^{core} as a function of U for $\bar{n} = 0.6$ (red) and $\bar{n} = 0.7$ (green). (b2): The spatial structure of M_s with $\bar{n} = 0.7$ and $U = 3$.

the Van Hove singularity ($0.5 \lesssim \bar{n} < 1$). The profiles of M_s for the $p_x + ip_y$ -wave vortex state with AFM moment and the $d_{x^2-y^2} + id_{xy}$ -wave case with the FM moment are displayed in Fig. 4(a2),(b2). Fig. 4(a2) shows clear staggered AFM manner of M_s with slow decay while (b2) FM manner with exponential decay away from the core. Different from the charge density waves (CDW) with periodic modulations $4a$ in d -wave cuprates[12], we find the Friedel oscillation of the electron density for the AFM case. As expected, both the AFM and FM orders cause the double-peak splitting of the LDOS peaks around the vortex center due to the lifting of the spin up-down degeneracy as shown in Fig. 4(a3), (b3). Such splitting of the LDOS associated with the vortex bound states opens a symmetric ($p_x + ip_y$ -wave case) or asymmetric ($d_{x^2-y^2} + id_{xy}$ -wave case) subgap with respect to the Fermi level, which provides a remarkable signal for the STM probing of possible magnetic orderings in this material.

To summarize, we have investigated the novel vortex state of $\text{Na}_x\text{CoO}_2 \cdot y\text{H}_2\text{O}$ with two possible pairing symmetries realized in the 2D triangular lattice. Besides the intriguing spatial structure of the vortex, we also find signature in the electronic structure of the vortex state associated with different pairing symmetries. In the presence of strong on-site repulsion, we find frustrated AFM

state in the $p_x + ip_y$ -wave vortex state and a localized FM state in the $d_{x^2-y^2} \pm id_{xy}$ -wave case. The local electronic structure and induced magnetic orders in the vortex state might be observed by the microscopic STM[19] and the spatially resolved NMR[20] probes with high resolution.

In finalizing this Letter, we noticed that Zhu and Balatsky [21] addressed a similar issue with taking into account only the $d_{x^2-y^2} \pm id_{xy}$ -wave pairing. To our understanding, at least the following major considerations and conclusions are quite different from theirs: (i) we compared two superconducting states with different pairing symmetries and found that when $\bar{n} = 1.35$ [corresponding to the $\bar{n} = 0.65$ for $t > 0$ in their paper] the ground state is $p_x \pm ip_y$ -wave pairing state, rather than $d_{x^2-y^2} \pm id_{xy}$ state; (ii) we found the AFM order induced in the core of the $p_x + ip_y$ -wave vortex ($U = 5$) and localized FM order ($U = 3$) in the $d_{x^2-y^2} \pm id_{xy}$ -wave vortex and predict that the splitting of the LDOS peak by both of the magnetic orders; (iii) we chose the *triangular* vortex lattice matching the triangular CoO_2 lattice, with the vortex structure exhibiting the intriguing six-fold symmetry, while they studied the *square* vortex lattice.

We thank Y. Chen for useful discussions. This work was supported by the RGC grant of Hong Kong (HKU7075/03P), the 973-project of the Ministry of Science and Technology of China under Grant Nos. G1999064602, and the NSFC grants 10204011, 10204019, and 10021001.

* Electronic address: zwang@hkucc.hku.hk

- [1] K. Takada *et al.*, Nature **422**, 53 (2003).
- [2] P. W. Anderson, Science **235**, 1196 (1987).
- [3] G. Baskaran, cond-mat/0303572.
- [4] B. Kumar and B. S. Shastry, cond-mat/0304210.
- [5] Q.-H. Wang, D.-H. Lee, and P. A. Lee, cond-mat/0304377.
- [6] A. Tanaka and X. Hu, cond-mat/0304409.
- [7] D. J. Singh, cond-mat/03045332.
- [8] J. Ni and G.-M. Zhang, cond-mat/0305423.
- [9] T. Waki *et al.*, cond-mat/0306036.
- [10] Y. Kobayashi, M. Yokoi, and M. Sato, cond-mat/0306264
- [11] J.-X. Zhu and C. S. Ting, Phys. Rev. Lett. **87**, 147002 (2001).
- [12] J.-X. Zhu *et al.*, Phys. Rev. Lett. **89**, 067003 (2002); Y. Chen *et al.*, *ibid.* **89**, 217001 (2002); M. Takigawa, M. Ichioka, and K. Machida, *ibid.* **90**, 047001 (2003).
- [13] H. Sakurai *et al.*, cond-mat/0304503.
- [14] Y. Wang and A. H. MacDonald, Phys. Rev. B **52**, R3876 (1995); Q. Han *et al.*, *ibid.* **66**, 104502(2002).
- [15] If $t > 0$ \bar{n} should be changed to $2 - \bar{n}$. Correspondingly $p_x \pm ip_y$ -wave pairing symmetry is favored for $\bar{n} < 1$ while $d_{x^2-y^2} \pm id_{xy}$ -wave pairing state for $1 < \bar{n} < 1.5$.
- [16] C. Caroli, P. G. de Gennes, and J. Matricon, Phys. Lett. **9**, 307 (1964).
- [17] M. Matsumoto and R. Heeb, Phys. Rev. B **65**, 014504 (2001).

- [18] The present case is essentially different from the field-induced mixed $d_{x^2-y^2} + id'_{xy}$ -wave state, which is composed of both the $l_z = \pm 2$ components, as the field-induced subdominant $d'_{xy} \ll d_{x^2-y^2}$. [See, M. Franz and Z. Tesanović, Phys. Rev. Lett. **80**, 4763 (1998); Q. Han *et al.*, Phys. Rev. B **65**, 064527 (2002).]
- [19] S. H. Pan *et al.*, Nature (London) **413**, 282 (2001).
- [20] V. F. Mitrović *et al.*, Nature (London) **413**, 501 (2001).
- [21] J.-X. Zhu and A. V. Balatsky, cond-mat/0306253.